PCCP

Shape integrals for polar convex molecules

Jiří Janeček and Tomáš Boublík

Charles University in Prague, Faculty of Science, Hlavova 2030, 128 40, Prague 2, The Czech Republic. E-mail: boublik@natur.cuni.cz

Received 20th February 2003, Accepted 7th April 2003
First published as an Advance Article on the web 1st May 2003

The contributions of electrostatic forces to the second virial coefficient and thermodynamic functions of convex molecule fluids can be determined using the perturbation approach. Particular terms in the perturbation expansion are given by multi-fold integrals; these integrals can be expressed after factorization as a product of two parts–simple integrals in terms of variable distance and (at least) three-fold integrals in angular coordinates. The latter integrals (denoted as *J* integrals) characterize the effect of the shape of molecular cores on the electrostatic interactions. Within this paper, values of several *J* integrals were calculated for hard spherocylinders of different reduced lengths (or diameter) with six types of embedded electrostatic interactions: dipole–dipole, quadrupole–quadrupole, dipole–quadrupole, dipole–induced dipole, quadrupole–induced dipole and quadrupole–induced quadrupole. The different *J* integrals were determined as functions of shapes for (like and unlike) pairs of hard convex bodies and expressed in the form of rational functions. The theoretical predictions of the second virial coefficient are compared with the pseudo-experimental values determined in our laboratory; comparison indicates sufficiency of the suggested method to evaluate thermodynamic properties of polar compounds.

1 Introduction

The description of the equilibrium behavior of molecular fluids composed of non-spherical molecules with electrostatic interactions (due to the permanent dipole, quadrupole, *etc.*) forms the basic information for chemical engineering design of technological processes, including biotechnologies and environmental friendly processes (*e.g.* supercritical fluid extraction).

At present, two basic approaches to the description of such systems are important. Both of them are extensions of two well-known models which have been used for the description of non-polar molecular fluids: (i) the first one is based on the interaction site model. The given molecule is assumed to be a collection of interaction sites which correspond to atoms or groups of atoms. The total interaction pair potential is given as a sum of interaction energies between pairs of sites on different molecules.[1] Electrostatic forces result from interactions of partial charges ascribed to individual sites. An advantage of this molecular model is simplicity of the determination of the site–site distance in simulation processes. Alternatively, one assumes the electrostatic forces as the result of the interactions of the dipoles (multipoles) embedded in the center of the molecule. Several simulation data for this model are available including values of the second virial coefficient.[2–4] However, the one-to-one resemblance of the potential model and molecular structure often fades in the case of application to real systems.[5] (ii) The alternative way of modelling interactions of non-spherical molecules consists in considering the generalized Kihara pair potential.[6] In this case a hard convex core is ascribed to the studied molecule and the pair interaction is assumed to depend on the shortest surface–surface (s–s) distance between the cores. The main disadvantage of this model consists in difficult determination of the s–s distance in simulations while considerable simplifications are offered in the case of theoretical expressions.[7] The electrostatic interactions are modelled by considering *e.g.* the permanent dipole or other multi-poles to be embedded in a center of the studied molecule. Such a model was applied in several theoretical studies;[8,9] simulation results were also published.[10]

Methods to determine thermodynamic functions of polar non-spherical Kihara molecule fluids have been studied in our laboratory for several years. Inclusion of the electrostatic (ES) interactions to the formalism developed for the Kihara molecule fluids represents a serious problem because of the different functional dependence of the Kihara and ES interactions on the separation of the interacting pair. Originally this problem was solved by substituting the Gaussian overlap (GO) [11] for the Kihara potential; in the GO the interaction energy of two molecules is expressed in the same way as for electrostatic interactions—as a function of the separation between the centers (not *via* the shortest s–s distance). This fact makes it possible to factorize the integrals for the ES contributions into two parts, a simple integral over distance and the "shape" integral (over angular coordinates) which depends only on the type of ES interaction and the shape of the Gaussian ellipsoid. Disadvantages of the method consist in uncertainty of ascribing the Gaussian ellipsoid of revolution to the given convex body and correct extension of the method to the case of dissimilar pairs of convex molecules.

In our recent work,[12] an attempt was made to evaluate the shape integrals directly for hard prolate spherocylinders. Significant improvement in comparison with the use of the GO was found even in the case of the Kihara rod-like molecules with soft repulsions.

In this paper we complete the results for rod-like molecules (and bring some results for oblate molecules). Six different types of electrostatic interactions are considered for wide range of reduced lengths. Theoretical predictions are compared with numerical values of the second virial coefficient determined within this study.

2. Theory

The total pair potential of molecules with electrostatic interactions can be expressed as a sum of a contribution of dispersion forces and that due to electrostatic interactions[13]

$$u = u_o + u_{ES} \tag{1}$$

where u_o is the reference Lennard-Jones, HCB or Kihara potential and $u_{ES} = \sum_i u_i$ represents the involved electrostatic interactions, *e.g.* interactions between permanent (and induced) multipoles. Within this work we have restricted our interest to interactions between two dipoles (μ–μ), two quadrupoles (Q–Q) and dipole–quadrupole interaction (μ–Q) and the first three terms describing induced forces: dipole–induced dipole ($\mu\alpha\mu$), quadrupole–induced dipole ($Q\alpha\mu$) and quadrupole–induced quadrupole ($Q\alpha Q$).

The intermolecular potential of molecular fluids (and both its parts) depends on generalized coordinates of both molecules, $u = u(\boldsymbol{x}_1, \boldsymbol{x}_2)$, where $\boldsymbol{x}_j = (\boldsymbol{r}_j, \boldsymbol{\Omega}_j)$; $\boldsymbol{r}_j$ is the position vector of the center of molecule j and $\boldsymbol{\Omega}_j = (\theta_j, \phi_j, \chi_j)$ is its normalized vector of orientational coordinates, $\int \mathrm{d}\boldsymbol{\Omega}_j = 1$. In the case of rod-like molecules with the multipole coinciding with the molecular axis, the number of the orientational coordinates decreases to two angles, θ and ϕ.

The electrostatic potentials u_i are of the form

$$u_i = X_i r^{-n} \Phi_i(\boldsymbol{\Omega}_1, \boldsymbol{\Omega}_2) \tag{2}$$

Values of X_i and n and expressions for the angle-dependent functions Φ_i for considered types of interactions are listed in Table 1. The second virial coefficient in the case of the considered potential can be expressed as

$$\begin{aligned} B &= -\frac{1}{2V}\int (\mathrm{e}^{-\beta(u_o+u_{ES})} - 1)\mathrm{d}\boldsymbol{x}_1\mathrm{d}\boldsymbol{x}_2 = \\ &= -\frac{1}{2V}\int \left[\mathrm{e}^{-\beta u_o}\left(\prod_i^m \mathrm{e}^{-\beta u_i}\right) - 1\right]\mathrm{d}\boldsymbol{x}_1\mathrm{d}\boldsymbol{x}_2 = \\ &= -\frac{1}{2V}\int \left[\mathrm{e}^{-\beta u_o}\prod_i^m\left(\sum_{j_i=0}^{+\infty}\frac{(-\beta u_i)^{j_i}}{j_i!}\right) - 1\right]\mathrm{d}\boldsymbol{x}_1\mathrm{d}\boldsymbol{x}_2 = \\ &= B_o + \sum_{\{j_1 j_2 \cdots j_m\}} B^{(j)}_{j_1 j_2 \cdots j_m} \end{aligned} \tag{3}$$

where in the last row the summation is prescribed over all permutations $\{j_1 j_2 \ldots j_m\}$, $j = j_1 + j_2 + \ldots + j_m$ is the order of the term,

$$B_o = -\frac{1}{2V}\int (\mathrm{e}^{-\beta u_o} - 1)\mathrm{d}\boldsymbol{x}_1\mathrm{d}\boldsymbol{x}_2 \tag{4}$$

and

$$B^{(j)}_{j_1 j_2 \cdots j_m} = -\frac{1}{2V}\int \mathrm{e}^{-\beta u_o}\prod_i^m \frac{(-\beta u_i)^{j_i}}{j_i!}\mathrm{d}\boldsymbol{x}_1\mathrm{d}\boldsymbol{x}_2 \tag{5}$$

Although we wrote the electrostatic part of the intermolecular potential as a sum of several contributions, in many real systems this part is often determined with one leading type (*e.g.* for strongly dipolar molecules—halogen hydrides, haloalkanes ...—only the dipolar interactions are considered and higher multipoles can be neglected *etc.*). Moreover it can be shown that the terms satisfying $j_i = 0$ for $i \neq i_0$ (and $j_{i0} = j$) are considerably more significant than the others. Thus, within this work the 'cross' terms are not taken into account and the expansion (3) simplifies to

$$B = B_o + \sum_i \sum_j B_i^{(j)} \tag{6}$$

where j is the order of contribution and i denotes the type of ES interaction. The terms $B_i^{(j)}$ are given as (*cf.* ref. 14)

$$B_i^{(j)} = -\frac{1}{2V}\int \mathrm{e}^{-\beta u_o}\frac{(-\beta u_i)^j}{j!}\mathrm{d}\boldsymbol{x}_1\mathrm{d}\boldsymbol{x}_2 \tag{7}$$

This expression results from (5) by considering $j_i = j$ for interaction of type i and taking the other j_is equal to zero. Thus for instance for the js contribution due to dipolar interaction we can write

$$\begin{aligned} B^{(j)}_{j0\ldots0} = B^{(j)}_{\mu\mu} &= -\frac{1}{2V}\int \mathrm{e}^{-\beta u_o}\prod_i \frac{(-\beta u_i)^{j_i}}{j_i!}\mathrm{d}\boldsymbol{x}_1\mathrm{d}\boldsymbol{x}_2 = \\ &= -\frac{1}{2V}\int \mathrm{e}^{-\beta u_o}\frac{(-\beta u_{\mu\mu})^j}{j!}\frac{(-\beta u_{QQ})^0}{0!}\ldots\mathrm{d}\boldsymbol{x}_1\mathrm{d}\boldsymbol{x}_2 = \\ &= -\frac{1}{2V}\int \mathrm{e}^{-\beta u_o}\frac{(-\beta u_{\mu\mu})^j}{j!}\mathrm{d}\boldsymbol{x}_1\mathrm{d}\boldsymbol{x}_2 \end{aligned} \tag{8}$$

In the case of hard convex bodies (HCB) the pair potential is

$$u(s) = \begin{cases} \infty, & s \leq \sigma \\ 0, & s > \sigma \end{cases} \tag{9}$$

If we consider two convex bodies having mutual orientation $\boldsymbol{\Omega}_1$ and $\boldsymbol{\Omega}_2$ at contact, the distance of their centers can be regarded as a new quantity $\sigma_o(\boldsymbol{\Omega}_1, \boldsymbol{\Omega}_2)$ and the reduced distance of centers x can be introduced

$$x = \frac{r}{\sigma_o(\Omega_1, \Omega_2)} \tag{10}$$

It is evident that for $x < 1$ the two bodies overlap, for $x > 1$ they do not and for $x = 0$ they are at contact. Thus, the definition of HCB potential (9) can be reformulated as

$$u(x) = \begin{cases} \infty, & x \leq 1 \\ 0, & x > 1 \end{cases} \tag{11}$$

With this definition of u_o, we can rearrange (7) to

$$\begin{aligned} B_i^{(j)} &= -\frac{1}{2}\int_0^\infty \int\int \mathrm{e}^{-\beta u_o}\frac{(-\beta X)^j}{j!} r^{-jn}[\Phi_i(\Omega_1, \Omega_2)]^j \\ &\quad \times 4\pi r^2 \mathrm{d}r\mathrm{d}\Omega_1\mathrm{d}\Omega_2 \\ &= -2\pi\sigma^3\frac{(-1)^j}{j!}\left(\frac{\beta X}{\sigma^n}\right)^j \int_0^\infty \int\int \mathrm{e}^{-\beta u_o} x^{-jn+2} \\ &\quad \times \left(\frac{\sigma_o(\Omega_1, \Omega_2)}{\sigma}\right)^{-jn+3}[\Phi_i(\Omega_1, \Omega_2)]^j \mathrm{d}x\mathrm{d}\Omega_1\mathrm{d}\Omega_2 \end{aligned} \tag{12}$$

Table 1 Survey of considered electrostatic interactions. In the first column are the labels for types of the interactions and in the next two the molecular characteristics of molecules 1 and 2 respectively are summarized. The Φ functions are expressed using a simplified designation: $c_1 = \cos\theta_1$, $c_2 = \cos\theta_2$, $s_1 = \sin\theta_1$, $s_2 = \sin\theta_2$ and $c_{12} = \cos(\phi_2 - \phi_1)$

i	1	2	X	n	Φ
μ–μ	μ_1	μ_2	$\mu_1\mu_2$	3	$2c_1c_2 + s_1s_2c_{12}$
μ–Q	μ_1	Q_2	$\frac{3}{2}\mu_1 Q_2$	4	$c_1(3c_2^2 - 1) + 2s_1s_2c_2c_{12}$
Q–Q	Q_1	Q_2	$\frac{3}{4}Q_1Q_2$	5	$1 - 5c_1^2 - 5c_2^2 - 15c_1^2c_2^2 + + 2(s_1s_2c_{12} - 4c_1c_2)^2$
$\mu\alpha\mu$	μ_1	α_2, κ_2	$-\frac{1}{2}\alpha_2{\mu_1}^2$	6	$(1 - \kappa_2)(3c_1 + 1) + 3\kappa_2(2c_1c_2 + s_1s_2c_{12})^2$
$Q\alpha\mu$	μ_1	α_2, κ_2	$-\frac{3}{2}\alpha_2\mu_1Q_1$	7	$4(1 - \kappa_2)3c_1^3 + 3\kappa_2(3c_1^2c_2 + 2c_1s_1s_2c_{12} - c_2)(2c_1c_2 + s_1s_2c_{12})$
$Q\alpha Q$	Q_1	α_2, κ_2	$-\frac{9}{8}\alpha_2{Q_1}^2$	8	$(1 - \kappa_2)(1 - 2c_1^2 + 5c_1^4) + + 3\kappa_2(3c_1^2c_2 + 2c_1s_1s_2c_{12} - c_2)^2$

Now the multi-fold integral can be decomposed into two parts

$$B_l^{(j)} = -2\pi\sigma^3 \frac{(-1)^j}{j!}\left(\frac{\beta X}{\sigma^n}\right)^j I_{jn}^{(j)} J_{jn}^{(j)} \tag{13}$$

where

$$I_{jn}^{(j)} = \int \mathrm{e}^{-\beta u_o} x^{-jn} x^2 \mathrm{d}x \tag{14}$$

is an integral that depends only on the form of u_o. In the case of HCBs $I_{jn}^{(j)} = \frac{1}{jn-3}$ for $jn > 3$. In similar way we can progress for other types of u_o; for $u_o = u_{LJ}$ the values of $I_{jn}^{(j)}$ are tabulated in wide ranges of reduced temperature and jn.[14]

The shape integral can be written as

$$\begin{aligned} J_{jn}^{i(j)} &= \int\int [\Phi_i(\Omega_1,\Omega_2)]^j \left(\frac{\sigma}{\sigma_0(\Omega_1,\Omega_2)}\right)^{jn-3} \mathrm{d}\Omega_1 \mathrm{d}\Omega_2 \\ &= \frac{1}{64\pi^4}\int_0^{\pi}\int_0^{\pi}\int_0^{2\pi}\int_0^{2\pi}\int_0^{2\pi}\int_0^{2\pi} [\Phi_i(\theta_1,\phi_1,\chi_1,\theta_2,\phi_2,\chi_2)]^j \\ &\quad \times \left(\frac{\sigma}{\sigma_0(\Omega_1,\Omega_2)}\right)^{jn-3} \sin\theta_1 \sin\theta_2 \mathrm{d}\theta_1 \mathrm{d}\theta_2 \mathrm{d}\phi_1 \mathrm{d}\phi_2 \mathrm{d}\chi_1 \mathrm{d}\chi_2 \end{aligned} \tag{15}$$

2. Results

3.1. Rod-like molecules

In the case of axially symmetric molecules with the multipole moments parallel to the main axis of symmetry the angles χ_1 and χ_2 become redundant and instead of two angles ϕ_1 and ϕ_2 only their difference $\phi_{12} = \phi_2 - \phi_1$ is sufficient to describe the mutual orientation of molecules. Thus, the relation (15) simplifies to

$$\begin{aligned} J_{jn}^{i(j)} &= \frac{1}{8\pi}\int_0^{\pi}\int_0^{\pi}\int_0^{2\pi} [\Phi_i(\theta_1,\theta_2,\phi_{12})]^j \\ &\quad \times \left(\frac{\sigma}{\sigma_o(\theta_1,\theta_2,\phi_{12})}\right)^{jn-3} \sin\theta_1 \sin\theta_2 \mathrm{d}\theta_1 \mathrm{d}\theta_2 \mathrm{d}\phi_{12} \end{aligned} \tag{16}$$

For calculation of the angularly dependent thickness $\sigma_o(\Omega_1,\Omega_2)$ (the distance of centers of molecules when the orientation of the first molecule is Ω_1, the other Ω_2 and the shortest separation of their cores is σ) a subroutine providing analytical results for every values of Ω_1 and Ω_2 was developed. Using numerical integration, integral $J_{jn}^{i(j)}$ can be evaluated for any combination of lengths of the core-rods L_1 and L_2

$$\begin{aligned} J_{jn}^{i(j)} &= \frac{1}{N_k N_l N_m}\sum_k^{N_k}\sum_l^{N_l}\sum_m^{N_m} [\Phi_i(\theta_1^{(k)},\theta_2^{(l)},\phi_{12}^{(m)})]^j \\ &\quad \times \left(\frac{\sigma}{\sigma_o(\theta_1^{(k)},\theta_2^{(l)},\phi_{12}^{(m)})}\right)^{jn+3} \sin\theta_1^{(k)} \sin\theta_2^{(l)} \end{aligned} \tag{17}$$

For $N_k = N_l = N_m = 120$ this simple method yields results good up to the fifth digit. Calculation of one such integral takes less than five minutes on the PC.

For six types of electrostatic interactions (μ–μ, Q–Q, μ–Q, $\mu\alpha\mu$, $Q\alpha\mu$ and $Q\alpha Q$) the first non-zero integrals were evaluated for the reduced lengths of cores $L = \{0,0.25,0.5,0.75,1.0,1.25,1.5,1.75,2.0,2.5,3.0,3.5,4.0,4.5,5.0\}$; thus, for each type of electrostatic interaction 225 values of J integral were obtained.

These results are tested using simulation values of the respective second virial coefficient. The simulation values of the second virial coefficient were obtained using the standard Monte Carlo integration in a rectangular box with the lengths of edges $10\sigma \times 10\sigma \times (10\sigma + 2l)$ (σ is length parameter of 12–6 potential and l is the length of the rod; a reduced scale $\sigma = 1$ was used and thus $L = l$). Particle 1 was fixed in the center of this box with the main axis of symmetry coinciding with axis z and the second particle was placed randomly into the box. The second virial coefficient is then given as

$$B = -\lim_{N\to\infty}\frac{V_{BOX}}{2N}\sum(\exp(-u(\boldsymbol{1},\boldsymbol{2})/kT) - 1) \tag{18}$$

where $\boldsymbol{1}$ and $\boldsymbol{2}$ denote the coordinates of molecules 1 and 2, V_{BOX} is the volume of simulation box and N is the number of configurations. For each studied type of molecules the total number of configurations was 5×10^8. From these configurations 10 values of virial coefficient were obtained and the average value and uncertainty interval were determined. Further increase of N did not cause any significant narrowing of the uncertainty interval.

During the simulation both parts of the pair potential, the 12–6 function and the electrostatic interaction, were truncated at the s–s distance $S_T = 5\sigma$ and c–c distance $R_T = 5\sigma$. Corresponding correction due to the truncation of the dipolar interaction was taken as

$$\Delta B^{\mu\mu} = -\frac{2\pi\sigma^3}{9T^{*2}}\left(\frac{\mu^2}{\varepsilon\sigma^3}\right)^2\left(\frac{\sigma}{R_T}\right)^3 \tag{19}$$

The analogous contribution for quadrupolar interaction

$$\Delta B^{QQ} = -\frac{2\pi\sigma^3}{5T^{*2}}\left(\frac{Q^2}{\varepsilon\sigma^5}\right)^2\left(\frac{\sigma}{R_T}\right)^7 \tag{20}$$

for considered values of $Q^2/\varepsilon\sigma^5$ is negligible similarly as the dipole–quadrupole contribution:

$$\Delta B^{\mu Q} = -\frac{\pi\sigma^3}{5T^{*2}}\left(\frac{\mu Q}{\varepsilon\sigma^4}\right)^2\left(\frac{\sigma}{R_T}\right)^5 \tag{21}$$

The correction for 12–6 interaction possesses a form

$$\begin{aligned} \Delta B^{12-6} &= \frac{2\pi\sigma^3}{3}\Delta f_3(T^*) + 4\pi R\sigma^2\Delta f_2(T^*) \\ &\quad + (S + 4\pi R^2)\sigma\Delta f_1(T^*) \end{aligned} \tag{22}$$

where

$$\Delta f_j(T^*) = 2^{-\frac{j}{6}}\int_{S_T}^{+\infty}\{1 - \exp[-(\varsigma^{-12} - \varsigma^{-6})/T^*]\}\mathrm{d}(\varsigma^j) \tag{23}$$

and R, S and V are geometrical functionals of the core. For $T^* = 1$ these integrals have the following values: −0.000256, −0.003200 and −0.031999.

The second virial coefficients in the case of hard oblate spherocylinders were determined by the same method. The size of the simulation box was decreased in a corresponding way and no corrections for 12–6 interaction were considered. The obtained results are listed in Tables 2, 3, 4 and 5.

In the case of μ–μ interaction, the integrals $J_3^{\mu\mu(1)}$ are exactly equal to zero due to properties of function $\Phi^{\mu\mu}$. Values of $J_3^{\mu\mu(2)}$ were evaluated for different lengths of molecules 1 and 2. Obtained results were interpolated for $(L_1, L_2) \in (0,5.0) \times (0,5.0)$ in the form of Padé approximant

$$J_6^{\mu\mu(2)} = \frac{a_6^{\mu\mu}(L_1) + b_6^{\mu\mu}(L_1)L_2 + c_6^{\mu\mu}(L_1)L_2^2}{1 + d_6^{\mu\mu}(L_1)L_2 + e_6^{\mu\mu}(L_1)L_2^2} \tag{24}$$

where the coefficeints $a_6^{\mu\mu}$, $b_6^{\mu\mu}$, $c_6^{\mu\mu}$, $d_6^{\mu\mu}$ and $e_6^{\mu\mu}$ are functions of L_1 also in the form of Padé approximants

$$x_6^{\mu\mu} = \frac{\alpha + \beta L_1 + \gamma L_1^2}{1 + \delta L_1 + \varepsilon L_1^2} \tag{25}$$

Values of $\alpha \ldots \varepsilon$ (here a does not mean the polarizability) are listed in Table 6; the coefficients for shape integrals $J_{10}^{QQ(2)}$ and $J_8^{\mu Q(2)}$ are also summarized in this table. This relatively complicated form correlates $J_6^{\mu\mu(2)}$ values with a precision of better than 5% (except several values for very long rods). In

Table 2 Simulation values of the second virial coefficient for dipolar Kihara rods with different lengths of core; $\mu^{*2} = 2$ and $T^* = kT/\varepsilon = 1.0$

B/σ^3				
L_2	$L_1 = 0$	$L_1 = 1.0$	$L_1 = 3.0$	$L_1 = 5.0$
0	-11.9 ± 0.1	-9.47 ± 0.08	-11 ± 0.1	-13.2 ± 0.1
0.5	-9.78 ± 0.07	-8.80 ± 0.09	-10.26 ± 0.09	-12.1 ± 0.1
1.0	-9.47 ± 0.08	-8.74 ± 0.06	-9.96 ± 0.08	-11.5 ± 0.1
1.5	-9.7 ± 0.1	-8.93 ± 0.09	-9.9 ± 0.1	-11.1 ± 0.1
2.0	-10.08 ± 0.08	-9.24 ± 0.08	-9.8 ± 0.1	-10.8 ± 0.1
2.5	-10.55 ± 0.09	-9.58 ± 0.08	-9.9 ± 0.1	-10.6 ± 0.1
3.0	-11.0 ± 0.1	-9.96 ± 0.09	-10.0 ± 0.1	-10.4 ± 0.2
3.5	-11.6 ± 0.1	-10.3 ± 0.1	-10.1 ± 0.1	-10.2 ± 0.1
4.0	-12.1 ± 0.1	-10.7 ± 0.2	-10.2 ± 0.1	-10.0 ± 0.2
4.5	-12.6 ± 0.1	-11.1 ± 0.2	-10.3 ± 0.2	-9.8 ± 0.2
5.0	-13.2 ± 0.1	-11.5 ± 0.1	-10.4 ± 0.2	-9.6 ± 0.2

Table 3 Simulation values of the second virial coefficient for Kihara rod-like molecules with quadrupole–quadrupole and dipole–quadrupole interaction. In the latter case L_1 represents the reduced length of molecule with dipole moment and L_2 the length of quadrupolar molecule; $T^* = 1.0$

B/σ^3				
	$Q^{*2} = 2$		$(\mu Q)^* = 3$	
L_2	$L_1 = 1.0$	$L_1 = 5.0$	$L_1 = 1.0$	$L_1 = 5.0$
1	-8.51 ± 0.05	-11.2 ± 0.1	-9.41 ± 0.09	-11.9 ± 0.1
2	-8.97 ± 0.09	-10.5 ± 0.1	-9.71 ± 0.06	-11.1 ± 0.1
3	-9.6 ± 0.1	-10.1 ± 0.1	-10.42 ± 0.06	-10.6 ± 0.1
4	-10.4 ± 0.1	-9.7 ± 0.2	-11.2 ± 0.1	-10.2 ± 0.2
5	-11.2 ± 0.1	-9.4 ± 0.2	-12.0 ± 0.1	-9.9 ± 0.2

Fig. 1 four sets of values of $J_6^{\mu\mu(2)}$ are plotted *vs.* the length of the second rod. The relative deviations of the approximated values from the exact values, $\Delta = (J_{\text{exact}} - J_{\text{app}})/J_{\text{exact}} \times 100\%$, %, for these sets are shown in Fig. 2.

In the case of rods of the same length $L_1 = L_2 = L$ $J_6^{\mu\mu(2)}$ and $J_{12}^{\mu\mu(4)}$ are expressed in the form of simple (3,3)-Padé approximants:

$$J_6^{\mu\mu(2)} = \frac{0.66667 + 0.06800L + 0.08041L^2}{1 + 1.95948L + 0.95300L^2} \quad (26)$$

$$J_{12}^{\mu\mu(4)} = \frac{0.96000 - 0.20424L + 0.47702L^2}{1 + 1.40311L + 34.40944L^2} \quad (27)$$

In Fig. 3 and 4 the MC values of the second virial coefficient for Kihara prolate molecules are compared with the prediction when only the first order contribution, $B^{(2)}$, is considered. A moderate value of the dipole moment $\mu_1\mu_2 = 2.0$ was chosen. Large differences for $L_1 = 0$ and $L_2 < 1$ (full line and circles in Fig. 3) are caused by the fact that in the case of two roughly spherical molecules the higher contributions are not small and thus negligible. Fig. 5 demonstrates the influence of involving higher order contributions containing $J_{12}^{\mu\mu(4)}$ to the values of the second virial coefficient of hard prolate spherocylinders; for three lengths $L = 0.5$, 1.0 and 2.0, the full lines represent the prediction with only the first order contribution, $B^{(2)}$, the dashed are calculated with both contributions, $B^{(2)}$ and $B^{(4)}$. The simulation data were taken from our previous work.[12] Significant improvement, especially for $L = 0.5$, is evident. For strongly non-spherical molecules the electrostatic forces play a less important role because of the lower values of J integrals.

Table 4 The pseudoexperimental second virial coefficient data for hard oblate spherocylinders with dipole moment perpendicular to main axis of symmetry

μ^{*2}	$D = 0.5$	$D = 1.0$
0	5.516	11.155
1	5.26 ± 0.01	11.03 ± 0.01
2	4.48 ± 0.01	10.64 ± 0.01
3	3.14 ± 0.01	9.98 ± 0.01
4	1.22 ± 0.01	9.05 ± 0.01

Table 5 The pseudoexperimental values of the second virial coefficient of Kihara oblate molecules with embedded dipole moment; $T^* = 1.0$

B/σ^3			
D	$\mu^{*2} = 1.0$	$\mu^{*2} = 2.0$	$\mu^{*2} = 3.0$
0.5	-8.47 ± 0.08	-10.9 ± 0.06	-14.6 ± 0.1
1	-7.70 ± 0.08	-8.8 ± 0.07	-10.4 ± 0.1
1.5	-5.96 ± 0.09	-6.6 ± 0.1	-7.5 ± 0.1
2	-2.4 ± 0.1	-2.8 ± 0.1	-3.4 ± 0.2
2.5	3.6 ± 0.2	3.3 ± 0.2	3.0 ± 0.3
3	12.6 ± 0.3	12.3 ± 0.3	12.1 ± 0.3

For prolate molecules with embedded quadrupole moment, the first integral $J_5^{QQ(1)}$ is not zero; nevertheless, the value of the corresponding contribution to the second virial coefficient is more than hundred times lower than the second contribution. The integrals $J_{10}^{QQ(2)}$ were approximated in the same way as $J_6^{\mu\mu(2)}$:

$$J_{10}^{QQ(2)} = \frac{a_{10}^{QQ}(L_1) + b_{10}^{QQ}(L_1)L_2 + c_{10}^{QQ}(L_1)L_2^2}{1 + d_{10}^{QQ}(L_1)L_2 + e_{10}^{QQ}(L_1)L_2^2} \quad (28)$$

and for $L_1 = L_2 = L$ more accurate relations were found:

$$J_{10}^{QQ(2)} = \frac{4.97778 - 0.40336L + 1.38863L^2}{1 + 4.33506L + 5.76639L^2} \quad (29)$$

$$J_{20}^{QQ(4)} = \frac{65.8429 - 10.0235L + 97.3912L^2}{1 - 29.5526L + 263.081L^2} \quad (30)$$

Fig. 6 shows three sets of $J_{10}^{QQ(2)}$ for representative lengths of rods and Fig. 7 their relative differences from the values of approximants. In Fig. 8 analogous comparison as in Fig. 3 and 4 is plotted for quadrupolar molecules.

Table 6 Coefficients of Padé approximants for $J_6^{\mu\mu(2)}$, $J_{10}^{QQ(2)}$ and $J_8^{\mu Q(2)}$

	α	β	γ	δ	ε
$a_6^{\mu\mu}(L_1)$	0.66667	+0.20828	+0.24205	+1.22131	+0.76335
$b_6^{\mu\mu}(L_1)$	0.20828	−0.12915	+0.02291	+0.45264	+0.03033
$c_6^{\mu\mu}(L_1)$	0.24205	−0.09551	+0.01257	+0.61310	−0.05889
$d_6^{\mu\mu}(L_1)$	1.22131	−0.24502	+0.14453	+0.00835	+0.10020
$e_6^{\mu\mu}(L_1)$	0.76335	−0.43981	+0.07763	−0.47333	+0.12223
$a_{10}^{QQ}(L_1)$	4.97778	+1.11184	+5.58378	+2.20887	+3.49185
$b_{10}^{QQ}(L_1)$	1.11184	−1.29856	+0.26654	+0.70020	+0.38342
$c_{10}^{QQ}(L_1)$	5.58378	−2.31487	+0.77908	+2.42221	+0.66511
$d_{10}^{QQ}(L_1)$	2.20887	−1.74669	+1.53638	+0.65997	+0.68259
$e_{10}^{QQ}(L_1)$	3.49185	−2.05957	+0.65515	−0.24024	+0.21708
$a_8^{\mu Q}(L_Q)$	0.44444	+0.12298	+0.31753	+1.69484	+1.81062
$b_8^{\mu Q}(L_Q)$	0.12767	−0.09621	+0.02592	+1.33983	+0.80241
$c_8^{\mu Q}(L_Q)$	0.27581	−0.04187	+0.11349	+2.01702	+3.49721
$d_8^{\mu Q}(L_Q)$	1.79290	−0.71266	+3.41415	−0.12621	+2.08475
$e_8^{\mu Q}(L_Q)$	1.67319	−1.03147	+1.32513	+0.18459	+1.38403

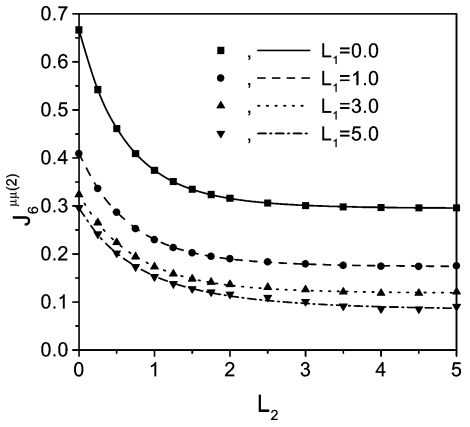

Fig. 1 Values of $J_6^{\mu\mu(2)}$ for different lengths of rods.

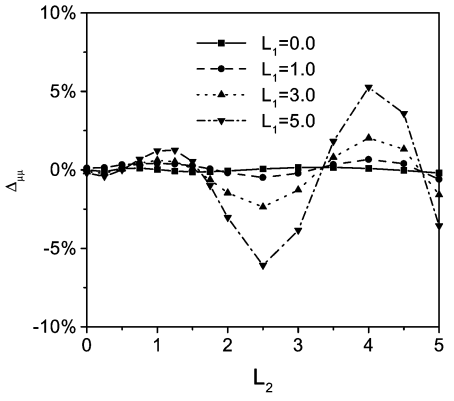

Fig. 2 Differences of the values of $J_6^{\mu\mu(2)}$ from the approximated values for the same sets of lengths as in Fig. 1.

Finally for the dipole–quadrupole interaction

$$J_8^{\mu Q(2)} = \frac{a_8^{\mu Q}(L_Q) + b_8^{\mu Q}(L_Q)L_\mu + c_8^{\mu Q}(L_Q)L_\mu^2}{1 + d_8^{\mu Q}(L_Q)L_\mu + e_8^{\mu Q}(L_Q)L_\mu^2} \tag{31}$$

and for identical rods we found

$$J_8^{\mu Q(2)} = \frac{0.44444 - 0.01456L + 0.07292L^2}{1 + 3.12555L + 2.04380L^2} \tag{32}$$

$$J_{16}^{\mu Q(4)} = \frac{0.47689 - 0.13706 + 0.27326L^2}{1 - 1.13363L + 83.50043L^2} \tag{33}$$

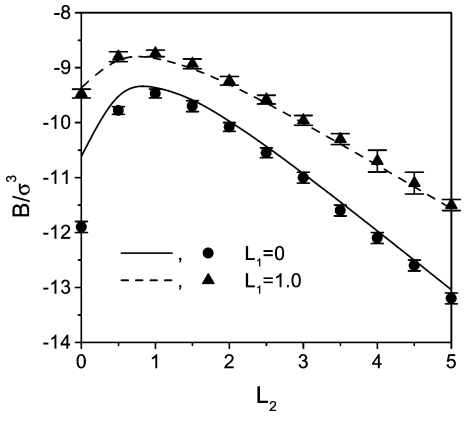

Fig. 3 The cross second virial coefficient for dipolar Kihara molecules for $L_1 = 0.0$ (full line and bullets) and $L_1 = 1.0$ (dashed line and triangles); $\mu_1\mu_2 = 2.0$.

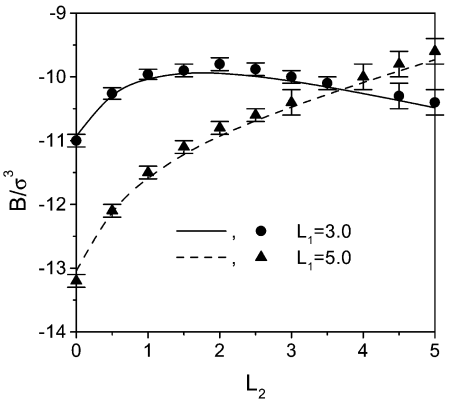

Fig. 4 The same as in Fig. 3 for $L_1 = 3.0$ (full line and bullets) and $L_1 = 5.0$ (dashed line and triangles); $\mu_1\mu_2 = 2.0$.

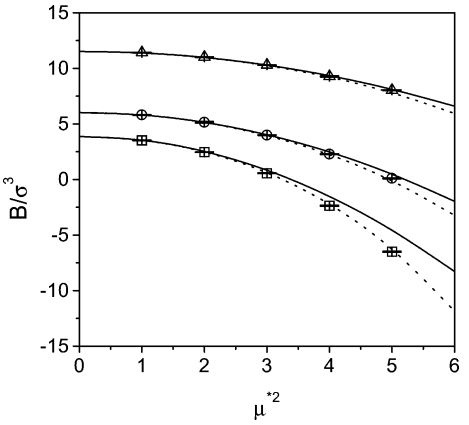

Fig. 5 The second virial coefficient for hard prolate spherocylinders of $L = 0.5$ (squares), 1.0 (circles) and 2.0 (triangles) *vs.* the dipole moment.

The pseudo-experimental results are compared with theoretical prediction in Fig. 9.

In the case of induced interactions the situations is more complicated because of one additional parameter—polarizability anisotropy κ_2—in the angular function Φ. This function can be for three considered induction interactions expressed as

$$\Phi = \Phi_A + \kappa_2\Phi_B \tag{34}$$

and this can be inserted into eqn. (5) and after some rearrangements we can write

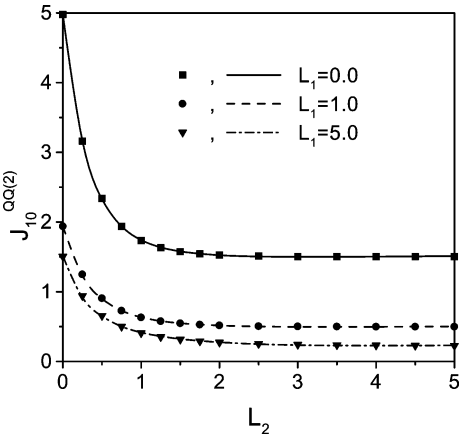

Fig. 6 Values of $J_{10}^{QQ(2)}$ for different lengths of rods.

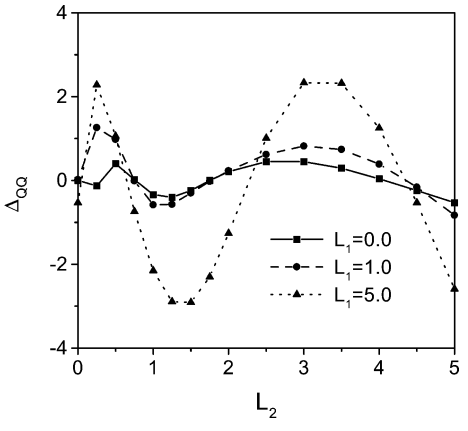

Fig. 7 Differences of the values of $J_{10}^{QQ(2)}$ from the approximated values for the same sets of lengths as in Fig. 5.

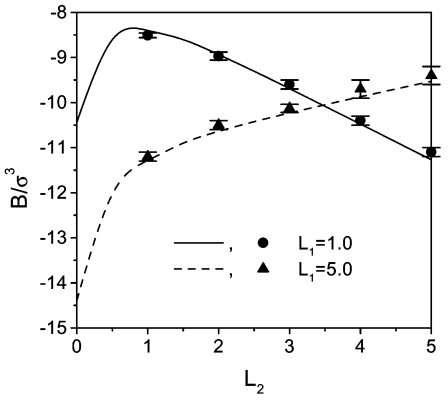

Fig. 8 The cross second virial coefficient for quadrupolar Kihara molecules for $L_1 = 1.0$ (full line and bullets) and $L_1 = 5.0$ (dashed line and triangles); $Q_1Q_2 = 2.0$.

$$J_{jn}^{i(j)} = \int\int (\Phi_A + \kappa_2\Phi_B)\left(\frac{\sigma}{\sigma_0(\Omega_1,\Omega_2)}\right)^{jn-3} \times d\Omega_1 d\Omega_2 = \sum_{i=0}^{j} A_i\kappa_2^i \qquad (35)$$

However in practical calculations the anisotropy of polarizability is usually taken as zero and thus the expression for $J_{jn}^{i(j)}$ reduces to $A_0 = J_0$.

For the dipole–induced dipole interaction, already the integral $J_6^{\mu\alpha\mu(1)}$ becomes non-zero and can be expressed as

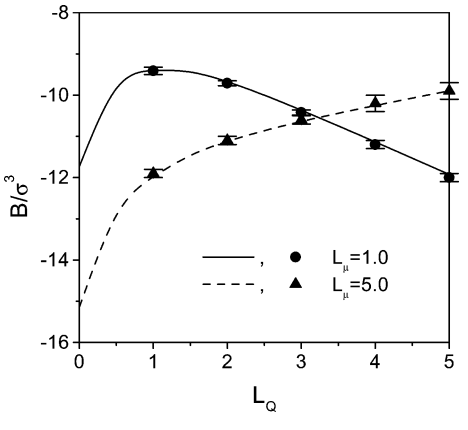

Fig. 9 The cross second virial coefficient for Kihara molecules with dipole–quadrupole interaction for $L_1 = 1.0$ (full line and bullets) and $L_1 = 5.0$ (dashed line and triangles); $\mu_1Q_2 = 3.0$.

$$J_6^{\mu\alpha\mu(1)} = J_0 + (J_1 - J_0)\kappa_2 = J_0(1-\kappa_2) + J_1\kappa_2 \qquad (36)$$

where

$$J_0 = \frac{a_0^{\mu\alpha\mu}(L_\alpha) + b_0^{\mu\alpha\mu}(L_\alpha)L_\mu + c_0^{\mu\alpha\mu}(L_\alpha)L_\mu^2}{1 + d_0^{\mu\alpha\mu}(L_\alpha)L_\mu + e_0^{\mu\alpha\mu}(L_\alpha)L_\mu^2} \qquad (37)$$

and

$$J_1 = \frac{a_0^{\mu\alpha\mu}(L_\alpha) + b_1^{\mu\alpha\mu}(L_\alpha)L_\mu + c_1^{\mu\alpha\mu}(L_\alpha)L_\mu^2}{1 + d_1^{\mu\alpha\mu}(L_\alpha)L_\mu + e_1^{\mu\alpha\mu}(L_\alpha)L_\mu^2} \qquad (38)$$

In the case of the quadrupole–induced quadrupole interaction we obtained similar expressions

$$J_8^{Q\alpha Q(1)} = J_0 + (J_1 - J_0)\kappa_2 = J_0(1-\kappa_2) + J_1\kappa_2 \qquad (39)$$

with

$$J_0 = \frac{a_0^{Q\alpha Q}(L_\alpha) + b_0^{Q\alpha Q}(L_\alpha)L_Q + c_0^{Q\alpha Q}(L_\alpha)L_Q^2}{1 + d_0^{Q\alpha Q}(L_\alpha)L_Q + e_0^{Q\alpha Q}(L_\alpha)L_Q^2} \qquad (40)$$

and

$$J_1 = \frac{a_1^{Q\alpha Q}(L_\alpha) + b_1^{Q\alpha Q}(L_\alpha)L_Q + c_1^{Q\alpha Q}(L_\alpha)L_Q^2}{1 + d_1^{Q\alpha Q}(L_\alpha)L_Q + e_1^{Q\alpha Q}(L_\alpha)L_Q^2} \qquad (41)$$

The term $J_7^{Q\alpha\mu(1)}$ for the quadrupole–induced dipole interaction is equal to zero. The dependence on κ_2 of the next non-zero term, $J_{14}^{Q\alpha\mu(2)}$, is quadratic and thus it is expressible using three sets of Padé approximants. Because of the low significance of this contribution such a form would be too complicated and we confine to the case $\kappa_2 = 0$

$$J_{14}^{Q\alpha\mu(2)} = \frac{a_0^{Q\alpha\mu}(L_\alpha) + b_0^{Q\alpha\mu}(L_\alpha)L_Q + c_0^{Q\alpha\mu}(L_\alpha)L_Q^2}{1 + d_0^{Q\alpha\mu}(L_\alpha)L_Q + e_0^{Q\alpha\mu}(L_\alpha)L_Q^2} \qquad (42)$$

The dependence of $a_0^{\mu\alpha\mu}(L_\alpha)$, $b_0^{\mu\alpha\mu}(L_\alpha)\ldots d_0^{Q\alpha\mu}(L_\alpha)$, $e_0^{Q\alpha\mu}(L_\alpha)$ on the length of polarizable molecule is expressed in the same form as in the case of permanent interactions; the coefficients of Padé approximants are given in Table 7.

3.2. Oblate molecules

In the case of oblate molecules the direction of multipoles was considered to be perpendicular to the main axis of symmetry; this orientation corresponds to reality in many common polar molecules (*e.g.* chlorobenzene, heteroaromates *etc.*). For our models only μ–μ, Q–Q and μ–Q interactions were considered. Because we were not able to carry out the calculation of $\sigma_o(\boldsymbol{\Omega}_1, \boldsymbol{\Omega}_2)$ in an analytical way, it was determined by interpolation of the surface–surface distance, s, to zero. For evaluation of this distance between two oblate spherocylinders of identical diameters of the core, a subroutine described in ref. 15 was used. Due to complexity of this case, calculations became more time consuming. Evaluation of one value with sufficient accuracy takes about thirty minutes.

For three considered types of interactions the following functions of the reduced diameter $D(= d/\sigma)$ were found:

$$J_6^{\mu\mu(2)} = \frac{0.66667 + 0.00069D - 0.00179D^2}{1 - 2.49698D + 1.86382D^2} \qquad (43)$$

$$J_8^{\mu Q(2)} = \frac{0.44444 - 0.14529D + 0.02169D^2}{1 + 3.66491D + 6.01541D^2} \qquad (44)$$

$$J_{10}^{QQ(2)} = \frac{4.97778 - 2.85632D + 0.56688D^2}{1 + 4.43768D + 15.48756D^2} \qquad (45)$$

As a rule, deviations are less than 1%; in the case of dipolar interactions they do not exceed 0.1%. In Fig. 10 virial coefficients for hard oblate spherocylinders with diameters

Table 7 Coefficients of Padé approximants for $J_6^{\mu\alpha\mu(1)}$, $J_7^{Q\alpha Q(1)}$ and $J_16^{Q\alpha\mu(2)}$

	α	β	γ	δ	ε
$a_0^{\mu\alpha\mu}(L_\alpha)$	2.00000	+0.62567	+0.72521	+1.22255	+0.76224
$b_0^{\mu\alpha\mu}(L_\alpha)$	1.21248	−0.21277	+0.06627	+0.94516	+0.01002
$c_0^{\mu\alpha\mu}(L_\alpha)$	1.28489	+0.00969	+0.11161	+1.51920	+0.68770
$d_0^{\mu\alpha\mu}(L_\alpha)$	1.32819	+0.38922	−0.01383	+0.52938	−0.03767
$e_0^{\mu\alpha\mu}(L_\alpha)$	1.05519	−0.12575	−0.00216	+0.49994	−0.10265
$a_1^{\mu\alpha\mu}(L_\alpha)$	2.13294	+0.86806	+0.87534	+1.26179	+0.79629
$b_1^{\mu\alpha\mu}(L_\alpha)$	0.52197	−0.21620	+0.07003	+0.19648	+0.14183
$c_1^{\mu\alpha\mu}(L_\alpha)$	0.68092	−0.21327	+0.06918	+1.01575	+0.39352
$d_1^{\mu\alpha\mu}(L_\alpha)$	1.19931	−0.09397	+0.23275	+0.24833	+0.20948
$e_1^{\mu\alpha\mu}(L_\alpha)$	0.72078	−0.29123	+0.07432	+0.34696	+0.11479
$a_0^{Q\alpha Q}(L_\alpha)$	1.33333	+0.38232	+0.82772	+1.79110	+1.67382
$b_0^{Q\alpha Q}(L_\alpha)$	0.72956	−0.30411	+0.15767	+1.33932	+0.47711
$c_0^{Q\alpha Q}(L_\alpha)$	1.48424	−0.48597	+0.20478	+1.89208	+0.53230
$d_0^{Q\alpha Q}(L_\alpha)$	1.71156	−0.05822	+0.81172	+0.20615	+0.47167
$e_0^{Q\alpha Q}(L_\alpha)$	2.18296	−0.69521	+0.24960	+0.24936	+0.09863
$a_1^{Q\alpha Q}(L_\alpha)$	1.33305	+0.38233	+0.82780	+1.79106	+1.67410
$b_1^{Q\alpha Q}(L_\alpha)$	0.36825	−0.27326	+0.03351	+0.77180	+0.04765
$c_1^{Q\alpha Q}(L_\alpha)$	0.95316	−0.18001	+0.05752	+1.93360	+0.29804
$d_1^{Q\alpha Q}(L_\alpha)$	1.69292	+2.22180	−0.30811	+1.53406	−0.21745
$e_1^{Q\alpha Q}(L_\alpha)$	1.81193	−0.24038	−0.00186	+0.24559	−0.06433
$a_0^{Q\alpha\mu}(L_\alpha)$	2.28490	−1.65363	+0.53955	+3.21724	−11.61092
$b_0^{Q\alpha\mu}(L_\alpha)$	0.74156	−0.43546	+0.12635	+3.14258	+9.21047
$c_0^{Q\alpha\mu}(L_\alpha)$	8.05786	−5.45434	+1.41943	+3.15834	+19.06291
$d_0^{Q\alpha\mu}(L_\alpha)$	2.44722	+1.06348	+0.05783	+0.42211	0.0
$e_0^{Q\alpha\mu}(L_\alpha)$	9.67391	+10.30024	−1.14680	+2.33349	−0.20850

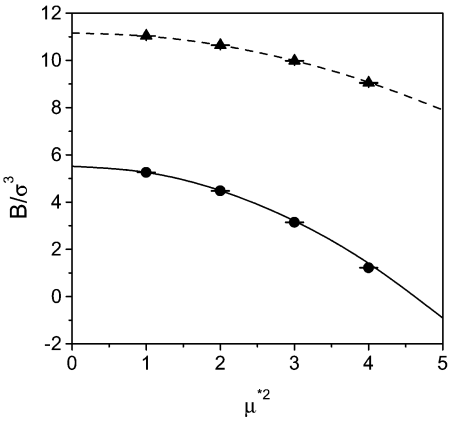

Fig. 10 The reduced second virial coefficient of dipolar hard oblate spherocylinders *vs.* the reduced dipole moment for two reduced diameters $-D = 0.5$ (full line + circles) and $D = 1$ (dashed line + triangles).

$D = 0.5$ and 1.0 are plotted. Fig. 11 shows the comparison of pseudoexperimental and theoretical values for the Kihara oblate molecules with $\mu^2 = 2.0$ and $\mu^2 = 4.0$. For higher diameters there is perfect agreement within the pseudoexperimental errors and thus only the interesting area is represented.

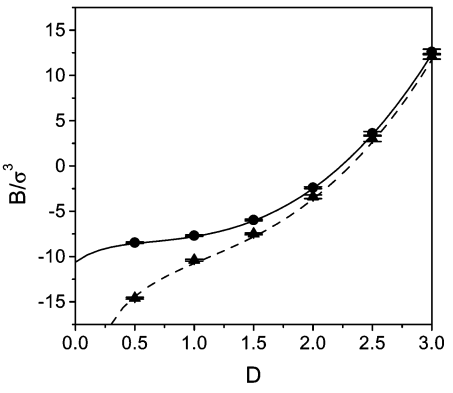

Fig. 11 The reduced second virial coefficient of dipolar Kihara oblate molecules *vs.* the reduced diameter D for two values of the dipole moment $\mu^{*2} = 2$ (bullets) and $\mu^{*2} = 4$ (triangles).

4. Conclusion

The J integrals for prolate molecules were expressed for six types of electrostatic interactions as functions of the reduced lengths of the cores. For oblate spherocylinders with permanent dipoles, quadrupoles and dipole–quadrupole interaction, the J integrals were evaluated and expressed in the form of rational functions for identical circles. For hard oblate spherocylinders as well as for the Kihara oblate molecules with permanent dipole moment several simulations of the second virial coefficient were performed. Sufficient accuracy of the used method and formulas was shown.

Acknowledgements

This work was supported by project MSMT 113100001 of the Ministry of Education of the Czech Republic and Grant No. 203/03/0282 of the Grant Agency of the Czech Republic.

References

1 J. O. Hirschfelder, C. F. Curtiss and R. B. Bird, *Molecular Theory of Gases and Liquids*, J. Wiley, New York, 1954.
2 A. Müller, J. Winkelmann, T. Boublík and J. Fischer, *Mol. Phys.*, 1993, **78**, 121.
3 C. Menduiña, C. McBride and C. Vega, *Phys. Chem. Chem. Phys.*, 2001, **3**, 1289.
4 C. Vega, C. McBride and C. Menduiña, *Phys. Chem. Chem. Phys.*, 2002, **4**, 3000.
5 P. Paricaud, A. Galindo and G. Jackson, *Fluid Phase Equil.*, 2002, **194**, 87.
6 T. Kihara, *Adv. Chem. Phys.*, 1963, **5**, 47.
7 T. Boublík, *Mol. Phys.*, 1976, **32**, 1737.
8 T. Boublík, *Mol. Phys.*, 1992, **76**, 327.
9 T. Boublík, *Mol. Phys.*, 1991, **73**, 417.
10 B. Garzón, S. Lago and C. Vega, *Mol. Phys.*, 1998, **96**, 123.
11 B. J. Berne and P. Pechukas, *J. Chem. Phys.*, 1972, **56**, 4213.
12 J. Janeček and T. Boublík, *Fluid Phase Equilibria*, submitted.
13 C. G. Gray and K. E. Gubbins, *Theory of Molecular Fluids. Volume 1: Fundamentals*, Clarendon, Oxford, 1984.
14 A. D. Buckingham and J. A. Pople, *Trans. Faraday Soc.*, 1955, **51**, 1173.
15 M. Wojcik and K. E. Gubbins, *Mol. Phys.*, 1984, **53**, 397.